ФИЗИКА

УДК 539.234:615.46:621.793.18:616.71-003.93 DOI: https://doi.org/10.54341/20778708_2026_3_68_11
EDN: VQVPRN

КОМПОЗИТНЫЕ АЭРОГЕЛИ НА ОСНОВЕ ХИТОЗАНА И ГИДРОКСИАПАТИТА, ПОКРЫТЫЕ КУРКУМИНОВОЙ ПЛЕНКОЙ, ДЛЯ ВОССТАНОВЛЕНИЯ ДЕФЕКТОВ КОСТНОЙ ТКАНИ

Цзипин Ван[1], Цзяхао Му[1], Мэнъян Пан[1,3], Сяосюэ Тан[1,3], Шанбинь Чжэн[2], Синь Лю[2], А. А. Рогачев[3], Сяохун Джанг[1]

[1]*Международная Китайско-Белорусская научная лаборатория физической химии и технологии биоматериалов, Нанкинский университет науки и техники*
[2]*Аффилированная больница китайской медицины Нанкинского университета*
[3]*Институт химии новых материалов Национальной академии наук Беларуси, Минск*

CURCUMIN-FILM-COATED CHITOSAN / HYDROXYAPATITE COMPOSITE AEROGELS FOR PERIODONTAL BONE DEFECT REPAIR PROPERTIES

Jiping Wang[1], Jiahao Mu[1], Mengyang Pang[1,3], Xiaoxue Tan[1,3], Shanbin Zheng[2], Xin Liu[2], A. A. Rogachev[3], Xiaohong Jiang[1]

[1]*International Chinese-Belarusian Scientific Laboratory of Physical Chemistry and Technology of Biomaterials, Nanjing University of Science and Technology*
[2]*The Affiliated Hospital of Nanjing University of Chinese Medicine*
[3]*Institute of Chemistry of New Materials of the National Academy of Sciences of Belarus, Minsk*

Аннотация. Пародонтит является основной этиологической причиной возникновения дефектов пародонтальных тканей. Однако традиционные материалы для восстановления костных дефектов пародонта обладают ограниченным набором функциональных свойств и не способны эффективно противостоять сложному микроокружению при пародонтите, что приводит к сохранению или рецидиву воспаления и формированию порочного круга репарация – инфицирование – повторная деструкция. Для преодоления этой проблемы в настоящей работе на основе хитозана и наногидроксиапатита, с использованием глутарового альдегида в качестве сшивающего агента, был получен композитный аэрогелевый матрикс хитозан/наногидроксиапатит. Структурно-фазовый анализ, морфологию и элементный состав полученного композитного аэрогеля исследовали с помощью методов ИК-Фурье (инфракрасная спектроскопия с преобразованием Фурье), РФА (рентгенофазовый анализ), РФЭС (рентгеновская фотоэлектронная спектроскопия) и РЭМ (растровая электронная микроскопия), а также провели тестирование антибактериальной активности, гемостатической способности и остеогенных свойств. Результаты показали, что композитный аэрогель хитозан/наногидроксиапатит обладает превосходной биосовместимостью и антибактериальной активностью. Кроме того, эксперименты in vitro продемонстрировали способность данного аэрогеля индуцировать остеогенную дифференцировку мезенхимальных стволовых клеток костного мозга крыс. Таким образом, разработанный композитный аэрогель на основе хитозана и наногидроксиапатита представляет значительный потенциал для применения в регенерации костных дефектов пародонта.

Ключевые слова: *хитозан*, *гидроксиапатит*, *аэрогель*, *структура*, *антибактериальная активность*.

Для цитирования: *Композитные аэрогели на основе хитозана и гидроксиапатита*, *покрытые куркуминовой пленкой*, *для восстановления дефектов костной ткани* / Цзипин Ван, Цзяхао Му, Мэнъян Пан, Сяосюэ Тан, Шанбинь Чжэн, Синь Лю, А. А. Рогачев, Сяохун Цзян // Проблемы физики, математики и техники. – 2026. – № 3 (68). – С. 11–17. – DOI: https://doi.org/10.54341/20778708_2026_3_68_11. – EDN: VQVPRN

Abstract. Periodontitis is the core cause of periodontal defects. However, the performance of traditional periodontal defect repair materials is single, which is difficult to cope with the complex microenvironment of periodontitis, leading to the persistence or recurrence of inflammation, and easy to form a vicious cycle of repair-infection-re-destruction. In order to solve the problem of single material performance, chitosan (CS) and nano- hydroxyapatite (nHAp) were used as raw materials, and glutaraldehyde (GA) was crosslinked with CS to obtain a chitosan/nano-hydroxyapatite (CS/nHAp) aerogel scaffold material. Curcumin (Cur) film was uniformly deposited on the surface of aerogel by low-power electron beam deposition (EBD) as an antibacterial functional layer to prepare a curcumin-chitosan/nano-hydroxyapatite (Cur-CS/nHAp) composite aerogel scaffold material. FTIR, XRD, XPS, SEM and other characterization methods were used to analyze the composition, structure and morphology of the composite aerogel, as well as the antibacterial, coagulation and osteogenic properties. The results show that it has excellent biocompatibility and antibacterial properties. In addition, in vitro experiments showed that Cur-CS/nHAp aerogel scaffolds could induce osteogenic differentiation of rBMSCs. The Cur-CS/nHAp aerogel scaffold prepared in this study has certain application potential in the repair of periodontal bone defects.

Keywords: *chitosan*, *hydroxyapatite*, *aerogel*, *structure*, *antibacterial activity*.

For citation: *Curcumin-film-coated chitosan/hydroxyapatite composite aerogels for periodontal bone defect repair properties* / Jiping Wang, Jiahao Mu, Mengyang Pang, Xiaoxue Tan, Shanbin Zheng, Xin Liu, A. A. Rogachev, Xiaohong Jiang // Problems of Physics, Mathematics and Technics. – 2026. – № 3 (68). – P. 11–17. – DOI: https://doi.org/10.54341/20778708_2026_3_68_11. – EDN: VQVPRN

© *Jiping Wang*, *Jiahao Mu*, *Mengyang Pang*, *Xiaoxue Tan*, *Shanbin Zheng*, *Xin Liu*, *A. A. Rogachev*, *Xiaohong Jiang*, 2026

1 Introduction

Periodontitis is an oral inflammatory disease caused by periodontal pathogens, affecting more than one billion people worldwide. It is the main cause of alveolar bone resorption, bone defect and tooth loosening in adults, and is associated with diabetes, obesity and depression [1]. The existing basic treatment can only remove plaque and control inflammation. However, surgical bone repair materials lack hemostatic, anti-inflammatory and antibacterial activities, and are difficult to adapt to irregular hemorrhagic defects, which can easily lead to postoperative bleeding, repeated infection and poor bone regeneration. Therefore, multifunctional bone repair materials with rapid hemostasis, anti-inflammatory, antibacterial, morphological adaptability and good biocompatibility are urgently needed.

Aerogel is a lightweight material with a three-dimensional interconnected porous network. It is widely used in bone defect repair due to its high porosity, large specific surface area and degradability [2]. Chitosan aerogel has good biocompatibility, can adsorb platelets to promote wound healing, and has natural antibacterial and hemostatic activities [3], but its mechanical strength is low, and its osteogenic induction and mineralization ability are insufficient. Hydroxyapatite is the main inorganic component of natural alveolar bone. It has excellent bone conduction and biomineralization ability [4]. It is recognized as an inorganic reinforcing material that can make up for the osteogenic defects of pure polymer aerogels [5]-[6]. Curcumin is a natural polyphenol with procoagulant, anti-inflammatory, antioxidant, broad-spectrum antibacterial and osteogenic activities [7]. It is safe to degrade in vivo, has low toxicity and does not produce drug resistance. It is an ideal active factor for full-cycle repair of periodontal defects.

In this study, EBD, a simple and controllable one-step film-forming method, was used to vaporize the target by electron beam under high vacuum to form a uniform, strong adhesion and controllable thickness film-Curcumin film was deposited on the surface of hydroxyapatite-loaded chitosan aerogel. The composite aerogel achieves full-cycle repair of antibacterial, hemostatic and bone regeneration, and provides a new multifunctional material for the clinical treatment of hemorrhagic bone defects caused by periodontitis.

2 Preparation and test method of composite aerogels

Nano-hydroxyapatite is prepared by hydrothermal method using $Ca(NO_3)_2{\cdot}4H_2O$ and Na_2HPO_4 under alkaline conditions. The chitosan powder is dissolved in acetic acid solution with a volume fraction of 2%, and then nano-hydroxyapatite suspensions with chitosan mass fractions of 0%, 5%, 10%, and 15% are added and stirred for 30 minutes. Then, an appropriate amount of glutaraldehyde solution is added to it, stirred for 30 minutes, then the free glutaraldehyde was removed by dialysis. Poured into the mold, and freeze-dried to obtain CS / nHAp aerogels, denoted as CS, CS / 5% nHAp, CS / 10% nHAp, CS / 15% nHAp, respectively. Subsequently, Cur powders with different mass (0.3g, 0.6g, 0.9g) are deposited on the surface of CS/nHAp aerogel by low power electron beam deposition. The final composite aerogels are recorded as 0.3Cur-CS / 10% nHAp, 0.6Cur-CS / 10% nHAp, 0.9Cur-CS / 10% nHAp, 0.6Cur-CS / 5% nHAp, 0.6Cur-CS / 15% nHAp, respectively. Chemical structure and physical structure test methods: The material structure and functional group characteristic peaks of raw materials and composite aerogels were analyzed by Fourier transform infrared spectrometer (FTIR, Thermo Fisher ICO LETIS10, USA). The curcumin film was characterized by infrared spectroscopy using potassium bromide tablets as the substrate. The phase composition and crystallinity of the composite aerogels were analyzed by X-ray diffractometer (XRD, D8ADVANCE-A-25, Germany). The X-ray is Cu-Kα, the diffraction wavelength is 0.154 nm, the voltage and current are 40 kV and 40 mA, respectively. The chemical structure and elemental composition of the films were analyzed by X-ray photoelectron spectroscopy (XPS, PHI Quantera II, Japan). Al Kα was used as a monochromatic X-ray source ($h\nu = 1486.6$ eV) and was measured on an XPS microprobe. BE correction is performed by the C1s peak (284.8 eV). The photoelectron line is approximated by a Gaussian function. The internal network structure of the aerogels was analyzed by scanning electron microscopy (SEM, Hitachi SU8600, Japan). The mechanical properties were characterized by universal mechanical testing machine (TY8000-A) of Jiangsu Tianyuan Test Equipment Co., Ltd. Each experiment was repeated three times, and the measurement data were presented as the mean ± standard deviation (Mean ± SD). In vitro biological performance test: Bone marrow-derived mesenchymal stem cells (rBMSCs) were used to evaluate the biological response of Cur-CS / nHAp aerogels. The sterile aerogel was immersed in complete medium (α-MEM + 10% FBS + 1% penicillin streptomycin) at 0.1 g/mL (w/v), and extracted at 37° C and 60 rpm for 72 h. The supernatant was centrifuged to remove particles to obtain 100% extract, which was immediately used for cell experiments, and the material-free medium under the same conditions was used as a blank control. The cells were cultured under standard conditions (37° C, 5% CO_2) in α-MEM supplemented with 10% fetal bovine serum and 1% gentamicin-penicillin mixture. During osteogenic differentiation experiments, cells were cultured in osteogenic

induction medium containing dexamethasone, β-glycerophosphate and ascorbic acid. The biocompatibility of the aerogels was evaluated by Calcein AM / PI live-dead staining. The sterilized aerogel extract was co-cultured with rBMSCs under standard culture conditions. After incubation, the cells were stained according to the manufacturer's procedures and observed using a fluorescence microscope. The evaluation of osteogenic differentiation is to evaluate the osteogenic differentiation ability of the composite aerogel by detecting the proteins related to bone formation (including transcription factor RunX2 and osteophosphoprotein (OPN)) by immuno-fluorescence staining. The cells cultured on the aerogel extract were fixed, permeabilized, incubated with specific primary antibodies, and then combined with fluorescent secondary antibodies. The nuclei were counterstained with DAPI, and the fluorescence intensity was semi-quantitatively analyzed. The antibacterial activity of the mineralized scaffold against Staphylococcus aureus and Escherichia coli was evaluated by agar diffusion method. The sterilized scaffolds were placed on LB agar plates inoculated with bacterial suspension and incubated at 37° C for 24 hours, and then the size of the inhibition zone was analyzed. All quantitative experiments were repeated independently. The data were presented as mean ± standard deviation (SD). Statistical analysis was performed using one-way analysis of variance (ANOVA), followed by appropriate follow-up tests.

The results of the chemical and physical structure and biological properties of the composite aerogels are shown in Figures 2.1–2.3.

Figure 2.1 shows the chemical structure of Cur-CS / nHAp composite aerogel. The components of CS / nHAp composite aerogels are analyzed by FTIR. As shown in Figure 2.1 (*a*), both pure CS aerogels and CS / nHAp composite aerogels demonstrate a new characteristic peak at 1638 cm^{-1}, which is due to the Schiff base reaction during the crosslinking process of aerogels. Because the asymmetric stretching vibration peak of phosphate at 1015cm^{-1} of nano-hydroxyapatite is similar to the asymmetric stretching vibration peak of C – O – C at 1152cm^{-1} of chitosan, the XRD analysis of CS / nHAp composite aerogel is carried out. As shown in Figure 2.1 (*b*), the diffraction peak of CS appears at 2θ of 20.35°, and the diffraction peaks of CS / nHAp composite aerogels are similar to those of CS. In addition, the diffraction peaks of nHAp appear in CS / nHAp composite aerogels, which proves that nHAp is successfully loaded in CS / nHAp composite aerogels, and no crystal change occurs after loading. At the same time, FTIR analysis is performed on the curcumin film deposited on the KBr sheet to explore the effect of EBD on the molecular structure of curcumin powder. Figure 2.1 (*c*) shows the FTIR spectra of Cur powder and Cur film. The peak of Cur powder at 3498 cm^{-1} corresponds to O – H bending, and the strong peak at 1626 cm^{-1} corresponds to C = O conjugation. In addition, the characteristic peaks at 1504 cm^{-1}, 1265 cm^{-1}, 1119 cm^{-1}, 957 cm^{-1} correspond to C = C vibration, O – CH_3 stretching vibration, C – O – C stretching vibration and C – H out-of-plane bending vibration, respectively. By comparison, it is found that the infrared characteristic peak of the film sample is more obvious and sharper than that of the powder sample. This is because compared with the powder, the Cur molecules in the film may have a certain orientation, thereby enhancing the infrared absorption of certain functional groups. The infrared spectrum of Cur film prepared by EBD method is slightly different from that of powder, but the characteristic functional groups are well preserved, indicating that the biological active components of Cur are basically unaffected.

In order to further verify the effect of EBD on the chemical structure of Cur powder and the successful doping of nHAp in CS / nHAp composite aerogel, XPS analysis is carried out. Figure 2.1 (*d*) shows the fitting analysis of C1s and O1s spectra of Cur powder and film. The C1s peak is composed of C – C(sp^2) / C – C bonds at 284.69 eV, C – OH / C – O – C / C – C(sp^3) bonds at 285.24 eV, C – OH / C – O – C bonds at 286.39 eV, and C = O bonds at 287.16 eV. The peak at 531.47 eV corresponds to the O – H bond, the peak at 532.79 eV corresponds to the C – O bond, and the peak at 533.42 eV corresponds to the C = O bond. It can be seen that the position and shape of the characteristic peaks of the Cur powder and the film are basically the same, indicating that the chemical structure of the film and the powder is similar. This result corresponds to the results of FTIR analysis, which again verifies that EBD preserves the chemical structure of Cur powder well and does not destroy its biological activity. Figure 2.1 (*e*) shows the XPS measurement spectra of the surface of blank CS aerogel and CS / nHAp composite aerogels deposited with different mass of Cur powder. The N1s content of CS is 5.3%, and the N1s on the surface of Cur-CS / nHAp composite aerogels is significantly reduced. This indicates that the Cur film successfully covers the aerogel, and as the thickness increases, the N element content almost disappears. In summary, curcumin films are successfully prepared on the surface of aerogels by EBD technology. Figure 2.1 (*f*) shows the XPS spectra of CS / nHAp composite aerogels doped with different contents of nHAp. It can be seen from the figure that with the increase of doping amount, the content of Ca and P elements gradually increases, and its atomic ratio is about 1.67, which conforms to the characteristic ratio of nHAp. In the C1s spectrum, the proportion of C – C gradually increases with the increase of nHAp content, but

nHAp does not contain C element. This is due to the strong adsorption capacity of nHAp, and the contaminated carbon carried by nHAp is included in C – C. In the O1s spectrum, the proportion of C – O gradually decreases with the increase of nHAp content, which is due to the presence of P – O in nHAp. In the Ca2p spectrum, the 2p orbital of the calcium element consists of two clearly separated double peaks of $Ca2p_{3/2}$ at 347.31 eV and $Ca2p_{1/2}$ at 350.88 eV. In the P2p spectrum, we can see the composition of $P2p_{3/2}$ at 132.94 eV and $P2p_{1/2}$ at 133.88 eV. In summary, nHAp is successfully doped into CS / nHAp composite aerogels, and the content of Ca and P elements gradually increases with the increase of doping amount.

The properties of Cur-CS / nHAp composite aerogels are affected by their surface morphology and internal network structure. Therefore, we observe the surface morphology and internal network structure of Cur-CS / nHAp composite aerogels. As shown in Figure 2.2 (*a*), the Cur-CS / nHAp composite aerogels are cylindrical and light in texture. The surface is yellow after being coated with curcumin, and the color increases with the increase of Cur content. Figure 2.2 (*b*) shows that the CS aerogel has a three-dimensional network structure that is interconnected and highly porous. After the addition of nHAp, the basic morphology of the aerogel remains unchanged, and its microstructure shows no signs of collapse, expansion or degradation. However, it can be observed that the pores of Cur-CS / nHAp aerogels are denser than those of CS aerogels. This is because nHAp is uniformly attached to the chitosan polymer chain, so that the thin-walled structure that is originally easy to collapse is supported, and the overall skeleton is more stable. For further verification, the mechanical properties of

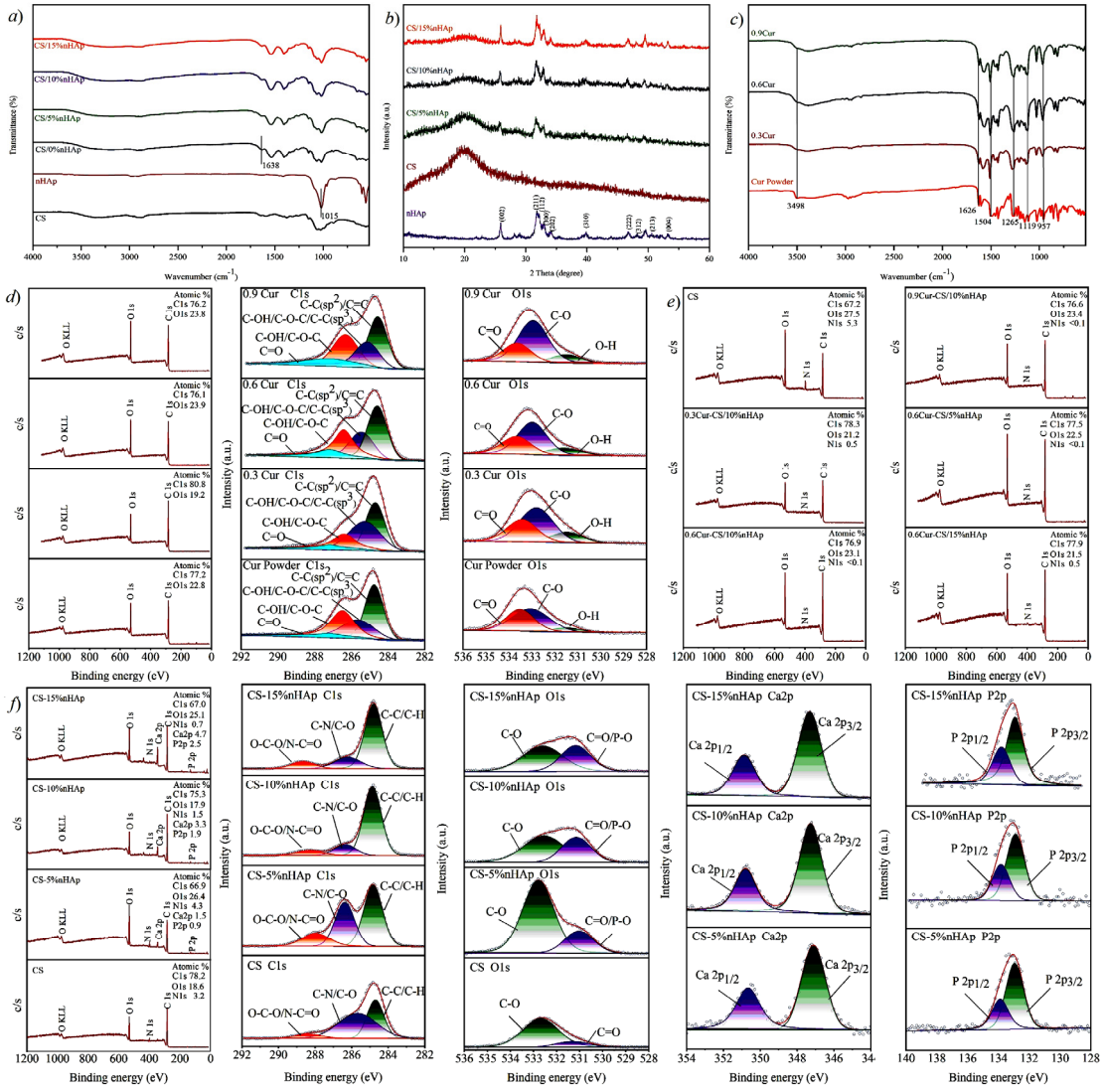


Figure 2.1 – Chemical structure analysis of aerogels (*a*) Infrared Spectra of CS, nHAp Powder and aerogel. (*b*) XRD patterns of CS, nHAp powder and aerogels. (*c*) Infrared Spectra of Cur Powder and Cur Film. (*d*) XPS spectra of curcumin powder and curcumin film. (*e*) XPS spectra of aerogel surface before and after coating Cur film. (*f*) The XPS spectra of CS and CS / nHAp aerogels

Cur-CS / nHAp aerogels are explored. Figure 2.2 (*c*) and Figure 2.2 (*d*) show the compressive stress-strain curve of Cur-CS / nHAp aerogel and the compressive stress and Young's modulus at 80% compressive strain. The results show that with the increase of the proportion of nHAp added to the aerogel, its mechanical properties also increase, which corresponds to the results of SEM. In addition, the appearance of Ca and P elements in the aerogel can be seen by EDS, which once again verifies the successful doping of nHAp.

Figure 2.3 shows the related biological properties of Cur-CS / nHAp composite aerogels. The effect of Cur-CS / nHAp composite aerogel on the viability of rBMSCs and the results of live / dead staining are shown in Figure 2.3 (*a*). After 24 hours of culture, rBMSCs grow well, and there are almost no dead cells (red) in each group. This is consistent with the results of CCK-8 test, indicating that Cur-CS/nHAp composite aerogel has no cytotoxicity to normal osteoblasts and can be used for in vivo implantation. The hemostatic properties of Cur-CS/nHAp composite aerogels in vitro are shown in Figure 2.3 (*b*). After the aerogel is exposed to 2 ml of fresh pig blood for 5 minutes, it can be observed that the coagulation effect of each experimental group is better than that of the control group, and 0.9Cur-CS / 10% nHAp has the best effect. Subsequently, its in vitro antibacterial properties are further explored, and the results are shown in Figure 2.3 (c).

Cur-CS / nHAp group has obvious inhibitory effect on *E. coli* and *S. aureus*. Among them, the 0.9Cur-CS / 10% nHAp group has the best effect, and the diameter of the inhibition zone against *E. coli* is about 3.6 cm, and the diameter of the inhibition zone against *S. aureus* is about 4.45 cm (see Table 2.1). It is worth noting that the antibacterial effect of 0.6Cur-CS / nHAp group is also very good, which is due to the fact that the doping amount of nHAp in this group is 15%. Related reports show that nHAp has a good antibacterial effect, especially for *S. aureus*[8]. In summary, the composite aerogel has excellent antibacterial properties and can effectively deal with the complex microenvironment of periodontitis.

Table 2.1 – The inhibition zone size of aerogels against *E. coli* and *S. Aureus*

	A	B	C	D	E	F
E. coli	1.99	2.53	3.24	3.6	2.95	3.4
S. aureus	2.32	2.85	2.95	4.45	2.5	4.24

In order to explore the osteogenic properties of Cur-CS / nHAp composite aerogels in vitro, RunX2 and OPN proteins are immunofluorescence stained and semi-quantitatively analyzed by ImageJ. As shown in Figure 2.3 (*d*), (*e*), the levels of RunX2 and OPN protein in the Cur-CS / nHAp group are higher than those in the CS group.

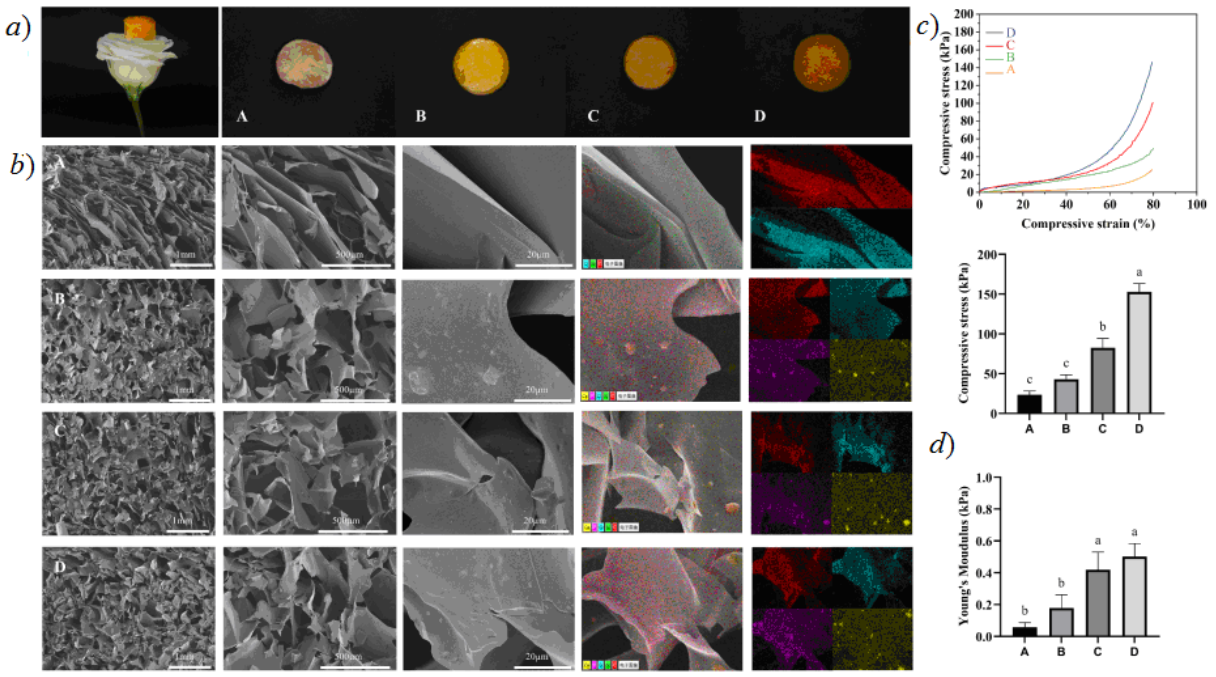


Figure 2.2 – Morphology and mechanical analysis of aerogels (*a*) Macroscopic morphology of aerogels. (*b*) The microstructure and EDS element analysis of aerogels. (*c*) Stress – strain test results of aerogels. (*d*) Young's modulus of aerogels. (A-CS, B-0.3Cur-CS / 5% nHAp, C-0.6Cur-CS / 10% nHAp, D-0.9Cur-CS / 15% nHAp). Different lowercase letters indicate significant differences among samples. Values are represented as average ± standard deviation (n = 3)

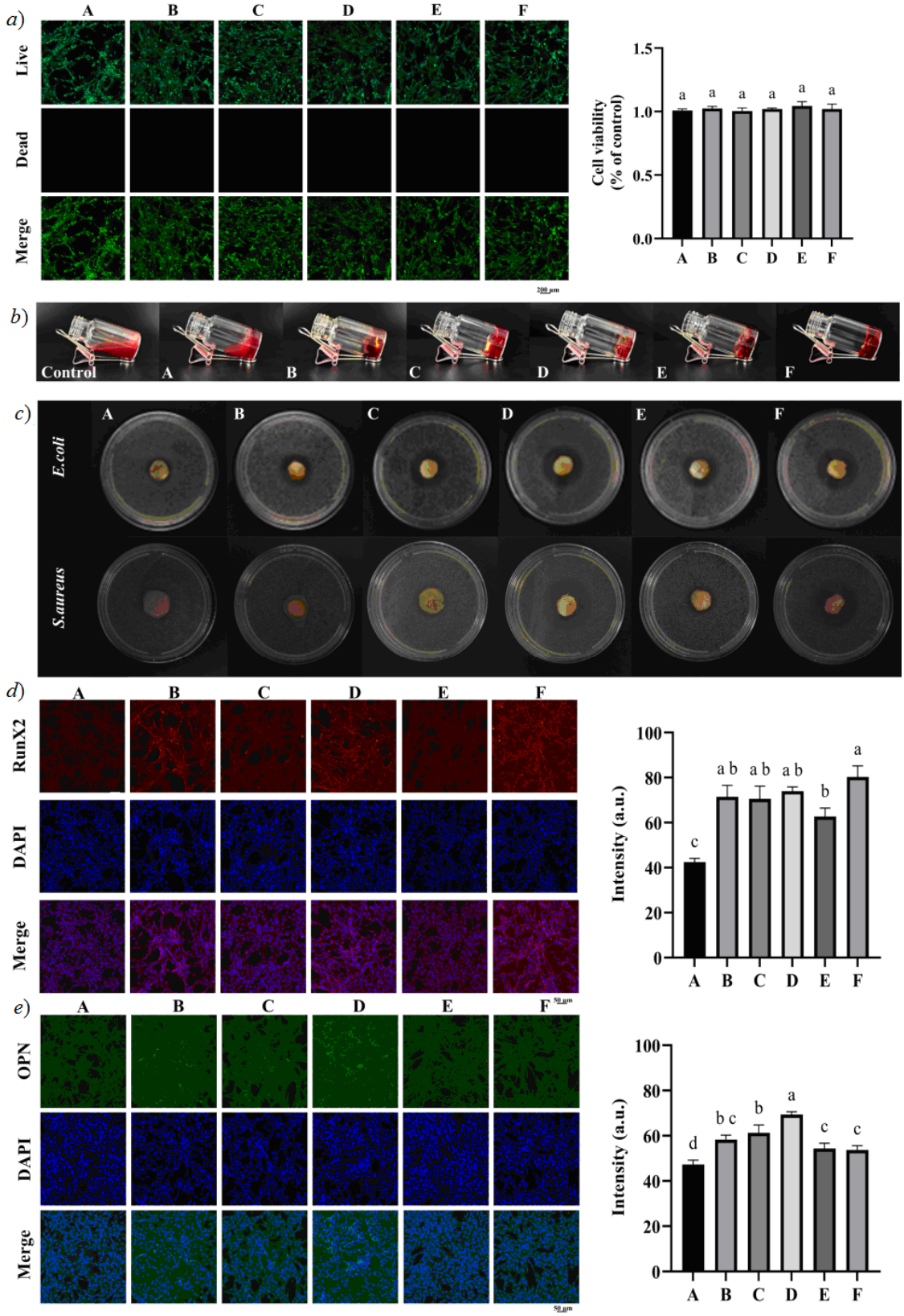


Figure 2.3 – Aerogel biological performance test. (*a*) Osteoblasts dead or alive. (*b*) Coagulation performance test. (*c*) antibiosis. (*d*) RunX2 fluorescence staining image and intensity. (*e*) OPN fluorescence staining image and intensity. (A-CS, B-0.3Cur-CS / 10% nHAp, C-0.6Cur-CS / 10% nHAp, D-0.9Cur-CS / 10%n HAp, E-0.6Cur-CS / 5% nHAp, F-0.6Cur-CS / 15% nHAp). Different lowercase letters indicate significant differences among samples. Values are represented as average ± standard deviation (n = 3)

It is worth noting that in Figure 2.3 (*e*), the OPN protein level decreases when the nHAp doping amount is 15% compared to 10%. This is because RunX2 is usually up-regulated in the early stage of induction, while OPN is a late marker. High levels of nHAp release more calcium and phosphorus ions, which may lead to the inability to effectively transcribe the downstream OPN gene, resulting in a decrease in OPN protein levels. In addition, it can be found from Figure 2.3 (*e*) that when the nHAp doping amount is constant, the expression level of OPN gradually increases with the increase of curcumin content [9]. In summary, Cur-CS / nHAp composite aerogels can synergis-tically promote the expression of osteogenic differentiation-related proteins, and the 0.9Cur-CS / 10% nHAp group has the best effect. Compared with the CS group, the RunX2 protein level is increased by 73.8%, and the OPN protein level is increased by 46.4%.

Conclusion

According to in vitro experiments, the Cur-CS / nHAp composite aerogel prepared in this experiment has good biological description performance and meets the basic requirements of bone tissue scaffolds for materials. The Cur film on its surface has excellent hemostatic and antibacterial properties, which can effectively inhibit the proliferation of bacteria around the periodontal tissue. In addition, its internal porous structure allows rBMSCs to adhere to the scaffold. At the same time, it has good biological activity and can promote the osteogenic differentiation of rBMSCs. In summary, the Cur-CS / nHAp aerogel scaffold has the structural characteristics and excellent biological properties, and has the potential to become a periodontal bone defect repair material.

REFERENCES

1. *Hajishengallis*, G. Local and systemic mechanisms linking periodontal disease and inflammatory comorbidities / G. Hajishengallis, T. Chavakis // Nature Reviews Immunology. – 2021. – Vol. 21, № 7. – P. 426–440.

2. *Insights into the role of biopolymer aerogel scaffolds in tissue engineering and regenerative medicine* / E. B. Yahya, A. A. Amirul, H. P. S. Abdul Khalil [et al.] // Polymers. – 2021. – Vol. 13, № 10. – P. 1612.

3. *Synthesis of hemostatic aerogel of TEMPO-oxidized cellulose nanofibers / collagen / chitosan and in vivo / vitro evaluation* / L. Liu, L. Liu, C. Chen [et al.] // Materials Today Bio. – 2024. – Vol. 28. – P. 101204.

4. *Features of alveolar ridge bone tissue regeneration using a hydroxyapatite-based material* / A. Yu. Drobyshev, N. A. Redko, E. G. Sviridov [et al.] // Traumatology and Orthopedics of Russia. – 2021. – Vol. 27, № 1. – P. 9–18 (in Russian).

5. *A chitosan-coated PCL / nano-hydroxyapatite aerogel integrated with a nanofiber membrane for providing antibacterial activity and guiding bone regeneration* / X. Deng, C. Yu, X. Zhang [et al.] // Nanoscale. – 2024. – Vol. 16, № 20. – P. 9861–9874.

6. *Synthetic biomaterials based on hydroxyapatite and tricalcium phosphate: an analysis of current clinical trials* / U. F. Mukhametov, D. S. Ivliev, I. F. Gareev [et al.] // Genij Ortopedii. – 2024. – Vol. 30, № 1. – P. 76–89 (in Russian)

7. *Astaneh*, *M. E*. Curcumin-loaded scaffolds in bone regeneration / M. E. Astaneh, F. Noori, N. Fereydouni // Heliyon. – 2024. – Vol. 10, № 11. – P. e32566.

8. *Alagl*, *A. S.* Antibacterial performance of biomimetic hydroxyapatite-functionalized titanium surfaces against Staphylococcus aureus and Escherichia coli: an in vitro study / A. S. Alagl, M. Madi // Frontiers in Oral Health. – 2026. – Vol. 7. – P. 1850878.

9. *Effective role of Curcumin on expression regulation of* EZH2 *histone methyltransferase as a dynamic epigenetic factor in osteogenic differentiation of human mesenchymal stem cells* / M. Ghorbaninejad, M. Khademi-Shirvan, S. Hosseini [et al.] // BBA – Gene Regulatory Mechanisms. – 2023. – Vol. 1866, № 1. – P. 194903.

The article was submitted 14.06.2026.

Information about the authors

Wang Jiping – Master's Student of School of Chemical Engineering

Mu Jiaohao – Master's Student of School of Chemical Engineering

Pang Mengyang – Master's Student of Institute of Chemistry of New Materials of the National Academy of Sciences of Belarus

Tan Xiaoxue – Doctor's Student of School of Chemical Engineering

Zheng Shanbin – Doctor's student of the Affiliated Hospital of Nanjing University of Chinese Medicine

Liu Xin – Chief Physician of the Affiliated Hospital of Nanjing University of Chinese Medicine

Rogachev Alexander Alexandrovich – Corresponding Member of the National Academy of Sciences of Belarus, Doctor of Engineering, Professor

Jiang Xiaohong – Professor